Defence Science Journal, Vol. 58, No. 1, January 2008, pp. 57-76


# Inverse Estimation of Time-varied Heat Flux and Temperature on 2-D Gun Barrel using Input Estimation Method with Finite-element Scheme

Tsung-Chien Chen and Chiun-Chien Liu

*Chung Cheng Institute of Technology, National Defense University*
*Tao Yuan, Taiwan-33509, R.O.C.*

**ABSTRACT**

When a gun fires, a large amount of heat flux is triggered by the propellant gas acting on the gun barrel inner wall, leading to the rise of temperature, which will cause serious destruction. In this paper, an inverse method based on the input-estimation method including the finite inverse heat conduction problem (IHCP) element scheme to inverse estimate the unknown heat flux on the 2-D gun barrel has been presented. The use of the online accuracy to inversely estimate the unknown heat flux on the chamber has been made using 7.62 mm gun barrel outer wall temperature measurement data. Using simulation uniform and non-uniform heat flux $q(z,t)$ cases involves a gun barrel inner wall that varies with time $t$ and the axial $z$-location with convection situation in the outer surface. Computational results show that the proposed method exhibits a good estimation performance and highly facilitates practical implementation.

**Keywords:** Heat flux, input-estimation method, finite element scheme, inverse heat conduction, inverse estimation

## NOMENCLATURE

| | |
|---|---|
| $B$ | Sensitivity matrix |
| $[C]$ | Capacitance matrix |
| $C_p$ | Specific heat |
| $[D]$ | Matrix of the conductivity values |
| $E$ | Elements number |
| $\{F\}$ | Thermal load vector |
| $H$ | Measurement matrix |
| $h$ | Convection heat transfer coefficient |
| $I$ | Identity matrix |
| $k$ | Time (discretised) |
| $K$ | Kalman gain |
| $K_b$ | Correction gain |
| $K_{rr}, K_Z$ | Thermal conductivity |
| $L$ | Length of $z$-direction |
| $M$ | Sensitivity matrix |
| $[M]$ | Global conductance matrix |
| $N$ | Total number of spatial nodes |
| $[N]$ | Shape function matrix |
| $P$ | Filter's error covariance matrix |
| $P_b$ | Error covariance matrix |
| $q$ | Heat flux |
| $Q$ | Process noise variance |
| $X$ | State vector |

Received 12 July 2006, revised 06 November 2006

| | |
|---|---|
| $z$ | Axial direction |
| $Z$ | Measurement data |
| $\alpha$ | Thermal diffusivity |
| $\gamma$ | Forgetting factor |
| $\Gamma$ | Input matrix |
| $\delta$ | Dirac delta function |
| $\rho$ | Density |
| $\Lambda,\Psi,\Omega,\Theta$ | Coefficient matrices |
| $\Phi$ | State transition matrix |
| $\{ff\},[G]$ | Coefficient matrix |
| $\sigma_{1,2,3....,\ n}$ | Standard deviation of the measurement noise |
| $\omega$ | Process noise vector |

*Subscripts*

| | |
|---|---|
| $1,2,\ldots,n$ | Sensor measurement location |
| $s$ | Body surface |

*Superscripts*

| | |
|---|---|
| $\bar{}$ | Estimated by filter |
| $\wedge$ | Estimated |
| $T$ | Transpose of matrix |
| $e$ | Element |
| $r$ | Axial direction |
| $R$ | Measurement noise variance |
| $R_i$ | Inner radial |
| $R_o$ | Outer radial |
| $s$ | Innovation covariance |
| $t$ | Time |
| $T$ | Temperature |
| $\{T\}$ | Temperature vector |
| $\Delta t$ | Sampling time interval |
| $v$ | Measurement noise vector |

**NOTATIONS**

| | |
|---|---|
| $\dot{\bar{\varepsilon}}$ | Effective strain rate |
| $\bar{\varepsilon}$ | Effective strain |
| $\beta$ | Temperature sensitivity term |
| $T$ | Temperature in absolute value |
| $\tau$ | Shearing stress |
| $\Omega$ | Contact surface between platen and tube |
| $D$ | Mean diameter of tube |
| $t$ | Thickness of tube |

## 1. INTRODUCTION

Gun barrel heating from multiple firings continues to be a subject of concern to ordnance engineers. Continuous gun firing raises the barrel temperature, producing several adverse effects on the system performance. In rapid firing situation, combustion gases and the projectile's sliding friction will produce chemical, mechanical, and temperature variations. The propellant gas temperature is the major factor to gun material melting, cracking, erosion, and wear[1-4], etc. The heat flux triggered by the propellant gas acts on the gun barrel chamber by way of thermal conduction. It leads to the high temperature effects to limit the performance of guns. It is suggested to use the outer surface temperature measurement to inversely estimate the unknown heat flux in the inner wall, which belongs to a hollow cylinder inverse heat conduction problem (IHCP). A number of investigators[5-11] have a sequence of discussions about heat transfer of gun tube. In these studies, the finite-difference scheme is used to solve the problem and described in detail in the 1-D problem. The heat flux variation in 2-D problem are seldom discussed. In this research, 2-D problem has been studied, and the heat flux $q(z\text{-}t)$ that varies with time and position has been discussed.

In this paper, an inverse-estimation method based on the input-estimation method including the finite element scheme, to inversely estimate the unknown heat flux on the 2-D gun barrel IHCP has been presented. The finite element discretisation concept has been applied to IHCP[12-14]. Irregularly

shaped boundaries can be approximated using elements with straight sides or matched exactly using elements with curved boundaries. Therefore, this method is not limited to regular shapes with easily defined boundaries in the future study. The input-estimation method uses the Kalman filter to generate the residual innovation sequence. A recursive least-squares algorithm is derived that uses this residual sequence to compute the value of the heat flux[15]. The proposed method for solving a 2-D gun barrel IHCP is also used for studying the modelling error effect and the temperature containing measurement errors. The uniform and non-uniform heat flux cases are simulated. These flux cases vary with time $t$ and the axial $z$-location with convection situation in the gun barrel outer surface. Then the sample time, model error, and measurement error are compared. The results demonstrate good performance and accuracy in tracking the unknown boundary heat flux $q(z,t)$ of a thermal system.

## 2. INPUT-ESTIMATION ALGORITHM

The recursive input-estimation algorithm consists of two parts, one is a Kalman filter and the other is a recursive least-squares algorithm. The input parameter is the unknown time-varying heat flux, the Kalman filter requires an exact knowledge of the process noise variance ($Q$) and the measurement noise variance ($R$), where $R$ depends on the sensor measurements. The Kalman filter is used to generate the residual innovation sequence. This recursive least-squares algorithm is derived by residual sequence to compute the value of the input heat flux.

The Kalman filter equations are given by

$$\bar{X}(k/k-1) = \Phi \bar{X}(k-1/k-1) + \Lambda h \tag{1}$$

$$P(k/k-1) = \Phi P(k-1/k-1)\Phi^T + \Gamma Q \Gamma^T \tag{2}$$

$$s(k) = HP(k/k-1)H^T + R \tag{3}$$

$$K(k) = P(k/k-1)H^T s^{-1}(k) \tag{4}$$

$$P(k/k) = [I - K(k)H]P(k/k-1) \tag{5}$$

$$\bar{Z}(k) = Z(k) - H\bar{X}(k/k-1) \tag{6}$$

$$\bar{X}(k/k) = \bar{X}(k/k-1) + K(k)\bar{Z}(k) \tag{7}$$

The Kalman filter is a time-varying digital filter, which uses information from both the state Eqns (1) and (6); embedded within the Kalman filter is a set of recursive matrix equations permitting the performance analysis of the filter before any data is processed, to precompute the state estimation-error covariance matrices prior to data processing is possible; $K(k)$ is the Kalman gain matrix, $P(k/k-1)$ is the state prediction-error covariance matrix, $P(k/k)$ is the state filtering-error covariance matrix, $\bar{X}(k/k-1)$ is the state filtering-error covariance matrix, $\bar{X}(k/k-1)$ is the recursive predictor and $\bar{X}(k/k)$ is the recursive filter.

Let $\hat{X}(k/k)$ and $\bar{X}(k/k)$ denote the estimate of $X(k)$ with and without unknown input $q(k\text{-}1)$.

$$\hat{X}(k/k-1)=\Phi\hat{X}(k-1/k-1)+\Lambda h+\Gamma q(k-1) \tag{8}$$

From Eqns (1) and (7), one gets:

$$\begin{aligned}\overline{X}(k/k)&=\overline{X}(k/k-1)+K(k)\overline{Z}(k)\\&=[I-K(k)H]\left[\Phi\overline{X}(k-1/k-1)+\Lambda h\right]+K(k)\overline{Z}(k)\end{aligned} \tag{9}$$

$$\begin{aligned}\hat{X}(k/k)&=\hat{X}(k/k-1)+K(k)[\hat{Z}(k)-H\hat{X}(k/k-1)]\\&=[I-K(k)H][\Phi\hat{X}(k/k-1)+\Lambda h+\Gamma q(k-1)]+K(k)\hat{Z}(k)\end{aligned} \tag{10}$$

Assume $q(k-1)$ is a constant at time interval, $k = n, n+1,..., n+l$.

$$q(k-1)=\left\{\begin{matrix}0,\ k<n\\q,\ n\le k\le n+l\end{matrix}\right\} \tag{11}$$

Equation (10)- Eqn (9), let $\Delta X = \hat{X}(k/k)-\overline{X}(k/k)$, then

$$\Delta X(k)=\left\{\begin{matrix}0,\ k<n\\[I-K(k)H]\left[\Phi\Delta X(k-1)+\Gamma q(k-1)\right],\ n\le k\le n+1\end{matrix}\right\} \tag{12}$$

Let $\Delta X(k) = M(k)\Gamma q$, and from Eqn (12)

$$M(k)=\left\{\begin{matrix}0,\ k<n\\[I-K(k)H]\left[\Phi M(k-1)+I\right],\ \ n\le k\le n+l\end{matrix}\right\} \tag{13}$$

$$\left\{\begin{matrix}\hat{X}(k/k)=\overline{X}(k/k), & k<n\\ \hat{X}(k/k)=\overline{X}(k/k)+M(k)\Gamma q, & n\le k\le n+l\end{matrix}\right. \tag{14}$$

$M(k)$ can be computed from Eqn (13).

Let $\hat{Z}(k)$ and $\overline{Z}(k)$ denote the residual sequence of measurement data with and without unknown input $q(k\text{-}1)$.

$$\begin{aligned}\overline{Z}(k)&=Z(k)-H\overline{X}(k/k-1)\\&=Z(k)-H\Phi\overline{X}(k-1/k-1)-H\Lambda h\end{aligned} \tag{15}$$

$$\begin{aligned}\hat{Z}(k)&=Z(k)-H\hat{Z}(k/k-1)\\&=Z(k)-H\Phi\hat{Z}(k-1/k-1)-H\Lambda h-H\Lambda q(k-1)\end{aligned} \tag{16}$$

Equation (15)- Eqn (16), and from Eqn (14), one can get a recursive relationship:

$$\overline{Z}(k)\begin{cases}\hat{Z}(k), & k<n\\ \hat{Z}(k)+B(k)q, & n\le k\le n+1\end{cases}$$

Here are the equations for a recursive least-squares algorithm. To understand the actual values, one can get[15]:

$$B(k)=H\left[\Phi M(k-1)+I\right]\Gamma \tag{17}$$

$$K_b(k)=\gamma^{-1}P_b(k-1)B^T(k)\left[B(k)\gamma^{-1}P_b(k-1)B^T(k)+s(k)\right]^{-1} \tag{18}$$

$$P_b(k)=\left[I-K_b(k)B(k)\right]\gamma^{-1}P_b(k-1) \tag{19}$$

$$\hat{q}(k)=\hat{q}(k-1)+K_b(k)\left[\overline{Z}(k)-B(k)\hat{q}(k-1)\right] \tag{20}$$

where $\hat{q}(k)$ is the estimated input vector, $P_b(k)$ is the error covariance of the estimated input vector, $B(k)$ and $M(k)$ are the sensitivity matrices, and $K_b$ is the correction gain. $\overline{Z}(k)$ is the bias innovation caused by the measurement noise and input disturbance. $s(k)$ is the covariance of the residual. $\gamma$ is a forgetting factor. $K(k)$, $s(k)$, and $\overline{Z}(k)$ are obtained from the Kalman filter. The correction gain $K_b(k)$ for updating $\hat{q}(k)$ in Eqn (20) is diminishing as $k$ increases, which allows $\hat{q}(k)$ to converge to the true constant value. In the time-varying case, however, one likes to prevent $K_b(k)$ from reducing to zero. This is accomplished by introducing the factor, $\gamma$. For $0<\gamma\le 1$, $K_b(k)$ is effectively prevented from shrinking to zero. Hence, the corresponding algorithm can preserve its updating ability continuously.

## 3. PROBLEM FORMULATION

For the hollow cylinder transient heat conduction problem, where $r$,θ,$z$ are the radial, circumferential, and axial axes, respectively. The temperature ($T$) is independent of the circumferential axis (θ). This is a case, where the domain is axisymmetric and all of the described boundary conditions are also axisymmetric. Therefore, the governing equation is simplified in two-dimensional, $R_i \le r \le R$, $0 \le z \le L$. The initial temperature is $T(r,z,0) = 0$. For time, $t > 0$ the boundaries at $z = 0$, $z = L$ are kept insulated and outer surface, $r = R_o$ is convection situation, convection coefficient is $h$ = 25 W /(m$^2$.$^o$C). The simulated measured temperatures $Z_m(t)$, $m$ =1,2,3... are known. The IHCP investigated here involves estimating heat flux input $\hat{q}_n(t)$, $n$=1,2,3... acting on the surfaces, $r = R_i$ in different position, respectively. To demonstrate the finite element method application to temperature distribution determination with a conducting body, Fig. 1 shows the geometry and discrete models. The mathematical formulation of the two-dimensional, transient, heat conduction problem can be generalised as

$$K_{rr}\frac{\partial^2 T}{\partial r^2}+\frac{K_{rr}}{r}\frac{\partial T}{\partial r}+K_{zz}\frac{\partial^2 T}{\partial z^2}=\rho C_p\frac{\partial T}{\partial t} \qquad R_i\le r\le R_0,\ 0\le z\le L,\ t>0 \tag{21}$$

$$T(r,z,0)=T_0=0 \qquad R_i\le r\le R_0,\ 0\le z\le L,\ t=0 \tag{22}$$

$$-K_{rr}\frac{\partial T}{\partial r}=q(z,t) \qquad r=R_i,\ 0\le z\le L \tag{23}$$

$$-K_{rr}\frac{\partial T}{\partial r}=h\left(T-T_{\infty}\right) \qquad r = R_0,\ 0 \le z \le L \tag{24}$$

$$\frac{\partial T}{\partial z}=0 \qquad R_i \le r \le R_0,\ z = 0 \tag{25}$$

$$\frac{\partial T}{\partial z}=0 \qquad R_i \le r \le R_0,\ z = L \tag{26}$$

$$Z_m(t) = T(R_0,z_m,t) + v(t) \qquad r = R_0,\ z = z_m,\ m = 1,2... \tag{27}$$

where $T_0$ is the uniform initial temperature, $q(z,t)$ is the unknown heat flux input to be estimated. There

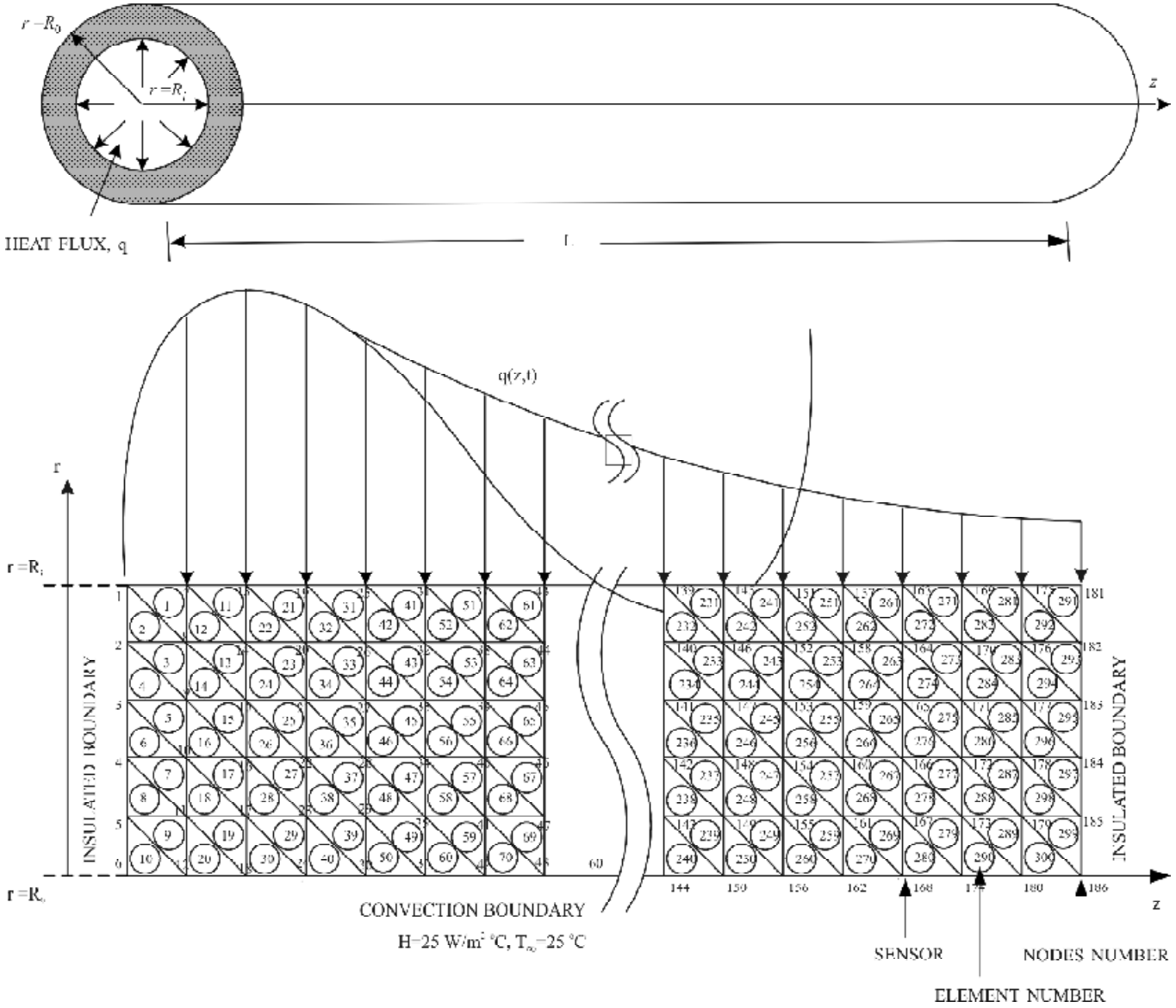


**Figure 1. Geometry and discrete models.**

is a non-uniform distribution at the $z$-axial, and $Z_m(t)$ are the noise-corrupted temperature measurements. $v(t)$ is the measurement noise assumed with zero mean and white Gaussian noise.

The calculus of variations provides an alternative method for formulating the governing Eqn (21) and boundary conditions [Eqns (23)-(26)]. Variational calculus states that the minimisation of the functional[16], can be written as

$$J = \frac{1}{2}\int\int\int_V \left[ K_{rr}\left(\frac{\partial T}{\partial r}\right)^2 + rK_{zz}\left(\frac{T}{z}\right)^2 + 2r\left(C_p\frac{T}{t}T\right)\right] dV - \int_{S_1}[qT]\,dS + \int_{S_2}\frac{1}{2}h(T - T_\infty)^2\,ds \tag{28}$$

$$\begin{aligned} J = {} & \sum_{e=1}^{E}\int_{V^e}\frac{1}{2}\{T\}^T\{B^e\}^T[D^e]\{B^e\}\{T\}dV + \int_{V^e} r\rho C_p[N^e]\{T\}[N^e]\frac{\partial\{T\}}{\partial t}dV \\ & + \int_{S_1^e} q_1[N^e]\{T\}\,dS + \int_{S_1^e} q_2[N^e]\{T\}\,dS + \int_{S_1^e} q_n[N^e]\{T\}\,dS \\ & + \int_{S_2^e}\frac{h}{2}\{T\}^T\{N^e\}^T\{N^e\}\{T\}\,dS - \int_{S_2^e} hT_\infty\{N^e\}\{T\}\,dS + \int_{S_2^e}\frac{h}{2}T_\infty^2 dS \end{aligned} \tag{29}$$

Equation (29) must be minimised wrt the set of nodal temperature values $\{T\}$.

$$\frac{\partial J}{\partial\{T\}} = \frac{\partial}{\partial\{T\}}\sum_{e=1}^{E} J^e = \sum_{e=1}^{E}\frac{\partial J^e}{\partial\{T\}} = 0 \tag{30}$$

When the minimisation process is complete, the following system of equations results[17]:

$$[C]\frac{\partial\{T\}}{\partial t} + [M]\{T\} + \{F\} = 0 \tag{31}$$

where Eqn (31) is a system of first-order linear differential equations. The element contributions to $[C]$, $[M]$, $\{F\}$ are summed in the usual manner.

$$[C]\sum_{e=1}^{E}[C^e] = \sum_{e=1}^{E}\int_V r\rho C_p[N]^T[N]dV \tag{32}$$

$$[M]\sum_{e=1}^{E}[M^e] = \sum_{e=1}^{E}\left(\int_V [B]^T[D][B]dV + \int_S h\{N\}^T\{N\}dS\right) \tag{33}$$

$$\{F\} = \sum_{e=1}^{E}[f^e] = \sum_{e=1}^{E}\left(\int_{S_1} q[N]^T dS + \int_{S_2} hT_\infty\{N\}dS\right) = [ff]\{q\} + [G].h \tag{34}$$

$[B]$ is obtained by differentiating $[N]$ wrt $r$ and $z$, and $[D]$ matrix consists of the conductivity values.

$q_n, n$ =1,2,3... are the unknown input heat flux at the inner wall, $r = R_i$ and the convection loss $h$ ($t$-$t_\infty$) at the outer wall, $r = R_o$ boundary. All of the integrals in Eqns (32)-(34) were evaluated over a single element. The element contributions are summed in the usual manner. From Eqn (31) and considering the process noise input, the continuous time state equation can be written as

$$\dot{T}(T) = \psi T(t) + \Omega[q(t) + \omega(t)] + \Theta h \qquad (35)$$

$$\Psi = (-1)[C]^{-1}[M]$$

$$\Omega = (-1)[C]^{-1}[ff]$$

$$\Theta = (-1)[C]^{-1}[G]$$

where the state vector $T(t)$ is $N \times 1$, $N$ is the total nodes, and $\Psi$, $\Omega$, and $\Theta$ are the coefficient matrices. $\omega(t)$ is a continuous time white-noise process. This noise term represents the modelling error.

Assume the state variable $(X)$ represents the temperature.

$$X=[T_1 \;\; T_2 \;\; T_3 \ldots \;\; T_{N-1} \;\; T_N]^T$$

$$X(k) = \Phi X(k-1) + \Gamma[q(k-1) + \omega(k-1)] + \Lambda h \qquad (36)$$

In general, one must compute $\Phi$, $\Gamma$ using numerical integration, and these matrices change from one-time interval to the next. The solution to state Eqn (35) can be expressed as

$$X(t) = \Phi(t,t_0)X(t_0) + \int_{t_0}^{t} \Phi(t,\tau)[\Omega(\tau)q(\tau) + \Omega(\tau)\omega(\tau)]\,d\tau + \int_{t_0}^{t} \Phi(t,\tau)[\Theta h]\,d\tau$$

where state transition matrix $\Phi(t,\tau)$ is the solution to the following matrix homogeneous differential equation:

$$\dot{\Phi}(t,\tau) = \Psi(t)\,\Phi(t,\tau) \qquad (37)$$

Next, one assumes that $q(t)$ is a piecewise constant function of time for $t \in [t_{k-1}, t_k]$ and set $t_0 = t_{k-1}$ and $t = t_k$ in Eqn (37), to obtain the values of the different matrices:

$$\Phi = e^{\Psi \Delta t} \cong I + \Psi \Delta t$$

$$\Gamma = \int_{t_{k-1}}^{t_k} e^{\Psi(t_k - \tau)} \Omega d\tau \cong \Omega \Delta t + \Psi \Omega \frac{\Delta t^2}{2} \cong \Omega \Delta t$$

$$\Lambda = \int_{t_{k-1}}^{k} e^{\Psi(t_k - \tau)} \Theta d\tau$$

$$q(k) = [q_1(k) \;\; q_2(k) \;\; q_3(k) \;\; .... \;\; q_n(k)]^T$$

where $X$ represents the state vector, $\Phi$ is the state transition matrix, $\Gamma$ is the input matrix, $\omega(k-1)$ is a discrete-time white-Gaussian sequence that is statistically equivalent through its first-two moments to

$$\omega(k-1) = \int_{t_{k-1}}^{t_{k+1}} \Phi(t_k, \tau)\Omega(\tau)\omega(\tau)\,d\tau$$

The mean and covariance matrices of $\omega(k-1)$ are:

$$E\{\omega(k-1)\} = E\left\{ \int_{t_{k-1}}^{t_k} \Phi(t_k, \tau)\Omega(\tau)\omega(\tau)\,d\tau \right\} = 0$$

$$E\{\omega(k)\;\omega^T(j)\} = Q\delta_{kj} = Q.I_{n \times n}.\delta_{kj}$$

where $\delta_{kj}$ is a Dirac delta function. Because, the measurements have been assumed to be available only at sampled values of $t$ at $t = t_i$, $i$=1,2,....,.To compare the results for situations involving measurement errors, one can express Eqn (27) as

$$Z(k) = HX_{exact}(k) + v(k) \qquad (38)$$

$$Z[Z_1 \;\; Z_2 \;\; Z_3 \ldots \;\; Z_M]^T$$

Equations (35) and (37) constitute the discretised state-variable model, where $X_{exact}$ is the solution

for the direct problem with a known $q(k)$, $Z$ is the measurement data at time $k\Delta t$, assumed to have zero mean and white noise. The variance of $v(k)$ is given by

$$E\{v(k)v^T(j)\} = R\delta_{kj} = \sigma^2\delta_{kj} = \sigma^2 . I_{n\times n} . \delta_{kj}$$

Figure 2 is the flow chart of the finite element including input-estimation algorithm.

## 4. RESULTS AND DISCUSSION

To illustrate the accuracy of the proposed approach in predicting the input heat flux $\hat{q}(K)$, *a* 2-D example is used to check the feasibility of the input-estimation method including the finite element scheme. The following physical quantities were used in the calculation:

Thermal properties of gun steel[19]

| Parameter | Values |
|---|---|
| Specific heat | $C_p$ = 460 J/(kg °C) |
| Density | ρ = 7,833 kg/m$^3$ |
| Thermal conductivity | $K_{rr}$ = $K_{zz}$ = 40 J/m.s.°C |
| Thermal diffusivity | α = 1.11×10$^{-5}$ m$^2$/s |

The total time is $t_f$, the sampling interval $\Delta t$ = 0.01s, and the unknown heat flux $q(z,t)$ is applied to the inner surface, $r = R_i$=0.00381 m, $0 \le z \le L$, $L$=0.30000 m. Thermocouples were placed in different nodes on the outer surface $r = R_o$=0.00381 m, respectively, elements number $E$ = 300, total number of spatial nodes $N$ = 186, the initial temperature $T_0$= 0, convection coefficient is $h$ = 25 W/m$^2$.°C. The above is a simulation of 7.62 mm gun under firing condition.

Because $P(-1/-1)$ and $P_b(-1)$ are normally unknown, the estimator was initialised with $P(-1/-1)$ and $P_b(-1)$ as very large numbers such as $10^{10}$ and $10^{10}$, respectively. $P$ is the error covariance of the estimated state and $P_b$ is the error covariance of the estimated input vector. This had the effect of treating the initial errors as very large. The estimator will therefore ignore the first few initial estimates[20]. The initial conditions for the input estimator were given by $\overline{X}(-1/-1)=[0\ 0\ ...0]^T$ and $P(-1/-1)=\text{Diag}[10^{10}]$ for the Kalman filter. The recursive least-squares algorithm initial conditions were given by $\hat{q}(-1)=[0\ 0\ ...0]^T$, $P_b(-1)=10^{10}.I_{nxn}$, and $M(-1)$ was set using a zero matrix. The Kalman filter for the recursive input-estimation algorithm requires exact knowledge of the process noise-variance matrix ($Q$) and the measurement noise-variance matrix $R$, where $R$ is dependent on the sensor measurements. The value of $Q$ in the filter from Eqn (2) and the value[21] of $\gamma$ = 0.8995 in the sequential least-squares from Eqn (18) approach interactively affect the fast adaptive capability for tracking the time-varying parameter. The test-input heat flux is given by

*Example* 1. Combined triangle and sine waveform in $q(t)$ (W/m$^2$). The input heat flux $q(t)$ is assumed in the form:

$$q(t)=\begin{cases} 0 & 0 \le t < 4, 12 < t < 20, 25 < t < t_f \\ 10^6 \times (t-4) & 4 \le t \le 8 \\ 10^6 \times (-t \times 12) & 8 \le t \le 12 \\ 2\times 10^6 \times (1+\sin[\overline{\omega}(t-20)]), \overline{\omega}=0.95, & 20 \le t \le 25 \end{cases} \quad (\text{W/m}^2) \qquad (39)$$

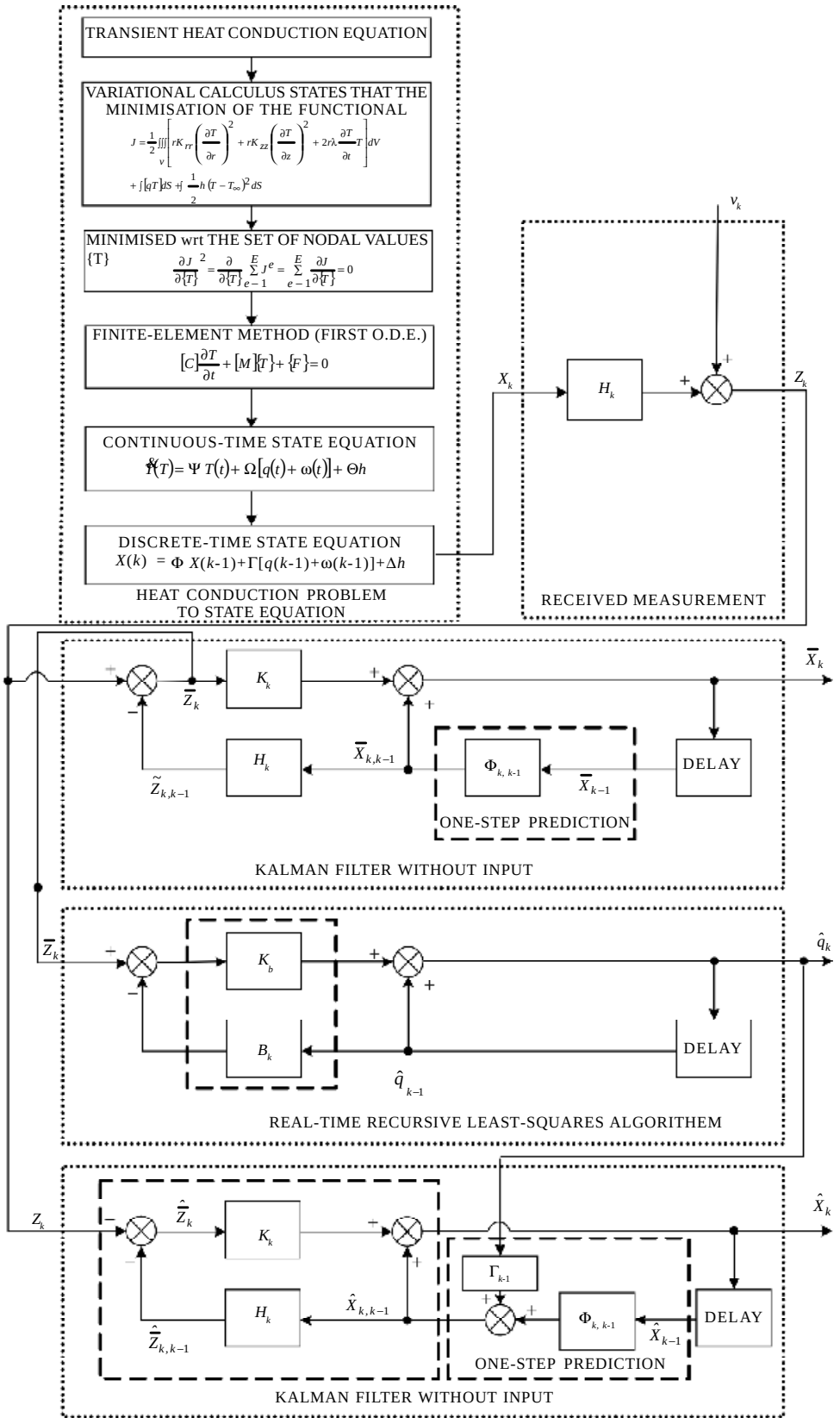


**Figure 2. Flow chart of the finite element including input-estimation algorithm.**

Firstly, consider the estimation input-heat flux, $q(t)$ is uniform on the boundary, $r = R_i$, at $z = 0$ and $z = L$ are kept insulated, the sensor location is at $r = R_0$, $z=L/2$ (node 96), elements number, $E$=300, the initial temperature $T_0$= 0, the sampling time interval $\Delta t = 0.01$ s, forgetting factor, $\gamma = 0.8995$, the outer wall surface is convection situation $h$ = 25 W/(m$^2$.$^o$C), $T_\infty$=25 $^o$C process noise covariance $Q$ = 1, and the measurement noise covariance, $\sigma$ = 0.0010, $\sigma$ = 0.0001. The estimates of $q(t)$ are shown in Figs 3-4 for $\sigma$ = 0.001and $\sigma$ = 0.0001, respectively. The outer wall temperature is shown in Fig. 5 and the convection effect in amplifying temperature scale in fig. 6. One can see the convection effect in Fig. 6. In this case, a uniform heat flux in every position is used to test this method. From Figs 3 and 4, one finds this method can estimate the unknown heat flux accuracy, and although the measurement error influences the estimate resolution, the results are still good.

*Example 2*. Five different levels input-heat flux are modelled by Weibull distribution form $q_n(z,t), \frac{(n-1)L}{5} \le z \le \frac{nL}{5}$, $n$ = 1,2,3,4,5 at the inner wall, $r = R_i$=0.00381 m assumed in the form:

$$q_i(z,t)=\begin{cases} 0 & 0 \le t < 2 \\ 2\times 10^7 \times e^{-z_i} \times \dfrac{b}{a}\left(\dfrac{t-2}{a}\right)^{b-1} \times e^{-\left(\frac{t-2}{a}\right)^b} & 2 \le t \le t_f \\ a = 4.8, b = 1.8 & i = 1,2,3,4,5 \\ z_1 = 1, z_2 = 1.5, z_3 = 2, z_4 = 2.5, z_5 = 3 & \end{cases} \quad (\mathrm{W/m^2}) \tag{40}$$

Here, simulate the unknown input heat flux $q(t)$ on the boundary. It is in a manner like the gun in firing with a large amount of heat flux from burning propellants in a short time. At $z = 0$ and $z = L$ are kept insulated with the sensors location at $r = R_0$, $z$ = node 24,60,96,132,168, elements number $E$ = 300, the initial temperature, $T_0$= 0, the sampling time interval, $\Delta t$ = 0.01s, forgetting factor $\gamma$ = 0.8995, convection situation, $h$ = 25 W/(m$^2$.$^o$C), $T_\infty$= 25$^o$C, process noise covariance, $Q$ = 1,10 and measurement noise covariance, $\sigma = 0.001, 0.0001$ . The estimates of $q(t)$ are shown in Fig 7-10, respectively.

Now, make a table about relative root-mean square-error with different parameters.

$\Delta t$($\Delta t_1$= 0.1s, $\Delta t_2$= 0.01s, $\Delta t_3$= 0.001s), $Q$($Q$ =1, $Q$ =10),

$R$($\sigma$ =10$^{-2}$, $\sigma$ =10$^{-3}$, $\sigma$=10$^{-4}$) as presented in Table 1.

The relative root-mean-square error (RRMSE) is defined[22] as

$$RRMSE = \sqrt{\frac{\sum_{i=1}^{n}\left[(q_{exact}(t_i) - \hat{q}_{est}(t_i)/q_{exact}(t_i)\right]^2}{n}} \tag{41}$$

From Figs 7-10, just as the measurement variance ($R$) increases, the Kalman gain [$K(k)$] Eqn (4) decreases. Kalman filter Eqn (7) is proportional to the difference between that measurement and its best predicted value and when the $\sigma$ increases, from Eqn (7) the Kalman gain [$K(k)$] decrease causes the estimate more believe-predicted value than new measurement. One can find that if the modelling error($Q$) from Eqns (2)-(4) increases, it will make $K(k)$ increase, which leads to estimation quickly in Figs 8 and 10. The sample time chosen must be small ($\Delta t_3$), but if the sample time is too large ($\Delta t_1$) the accuracy will decrease. In this case, from Table1, if one chooses the sample time ($\Delta t_2$), it can reach accuracy. From Figs 7-10 show that a larger measurement error can cause estimation lag and estimate accuracy

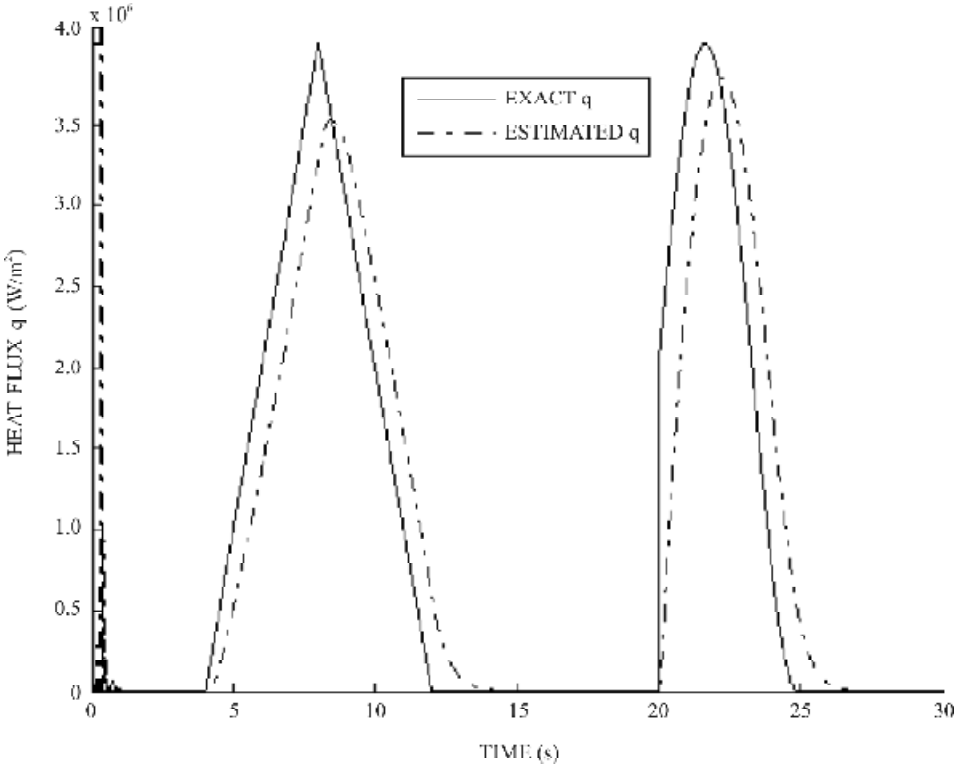


**Figure 3. Inverse estimation for $q(t)$ for example 1 with $\sigma = 0.0001$ and $Q = 1$.**

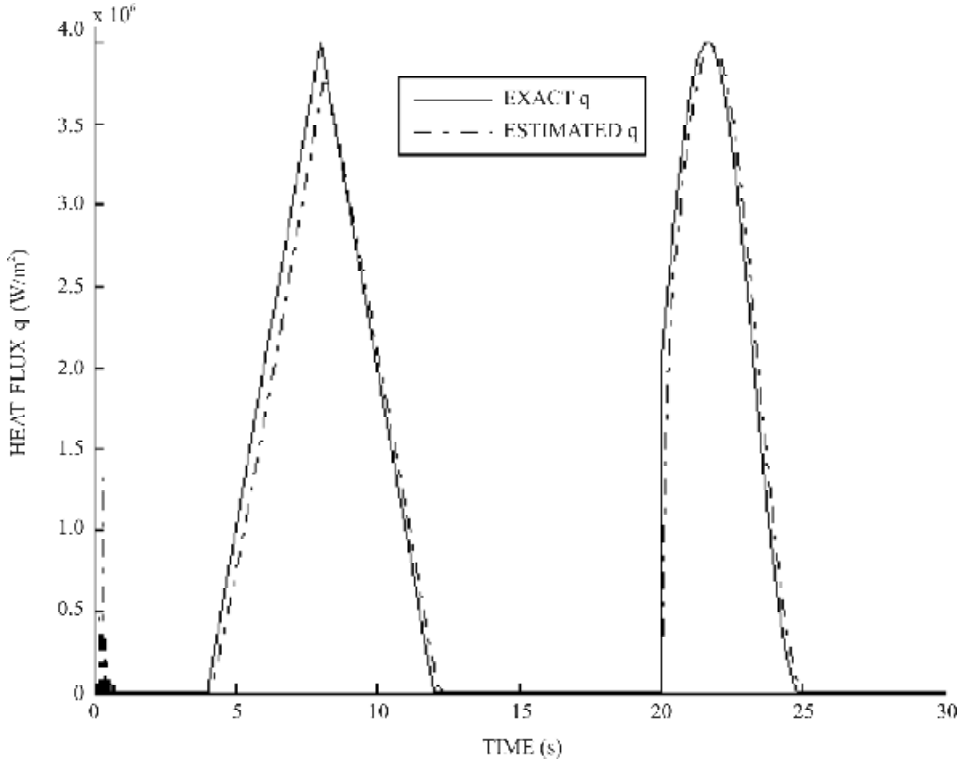


**Figure 4. Inverse estimation for $q(t)$ for example 1 with $\sigma = 0.001$ and $Q = 1$.**

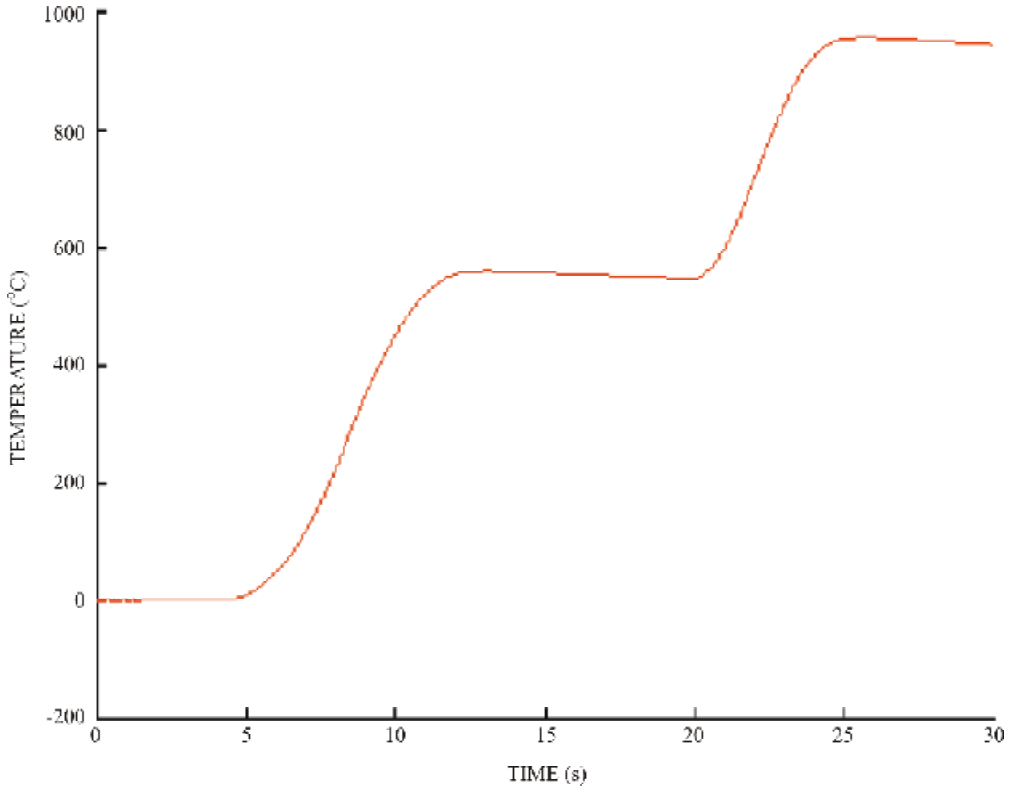


**Figure 5. Outer wall temperature for example 1.**

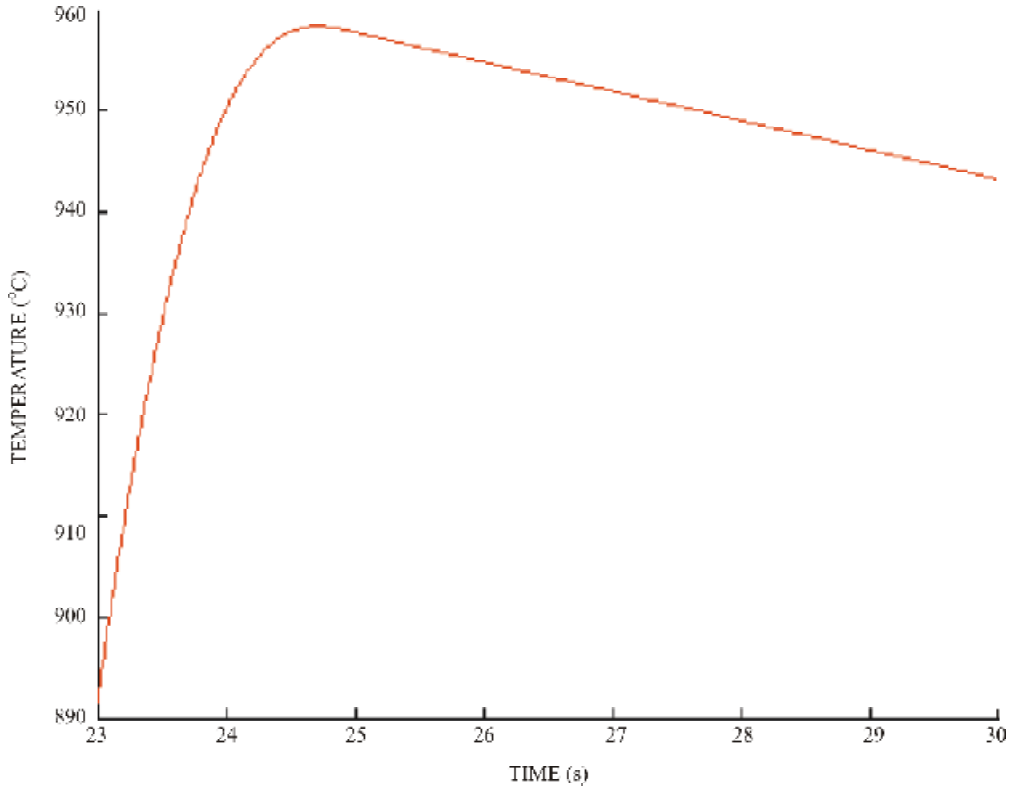


**Figure 6. Convection effect in amplifying temperature scale for example 1.**

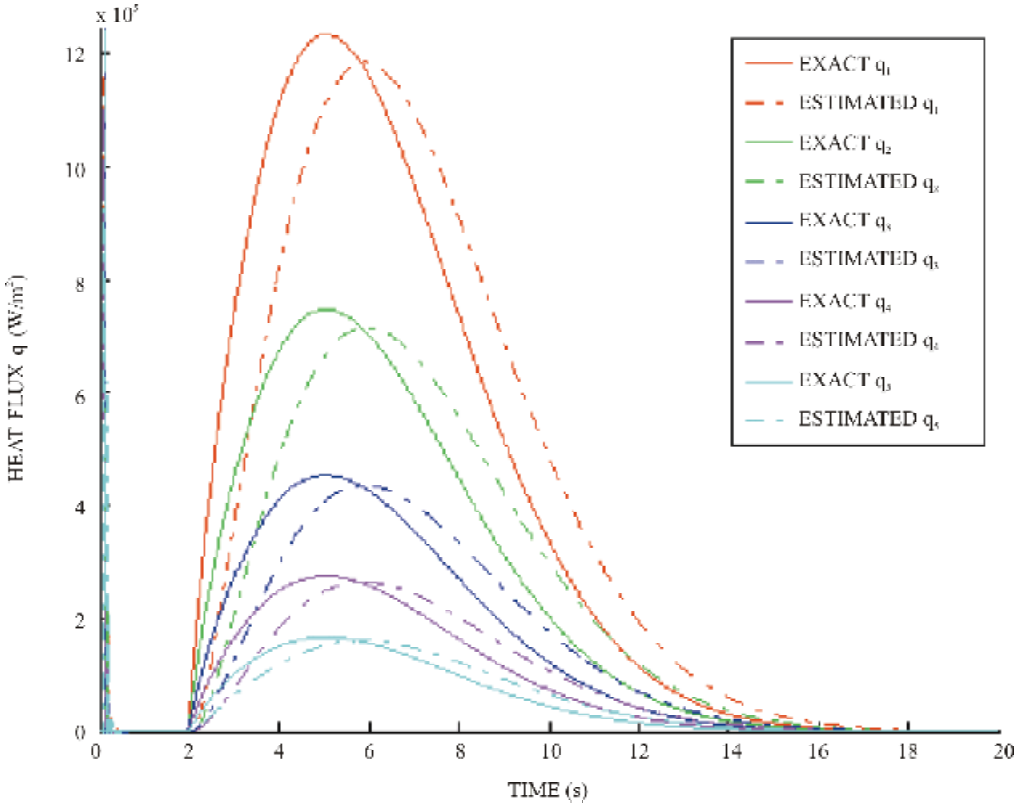


**Figure 7. Inverse estimation for $q(t)$ for example 2 with $\sigma = 0.001$ and $Q = 1$.**

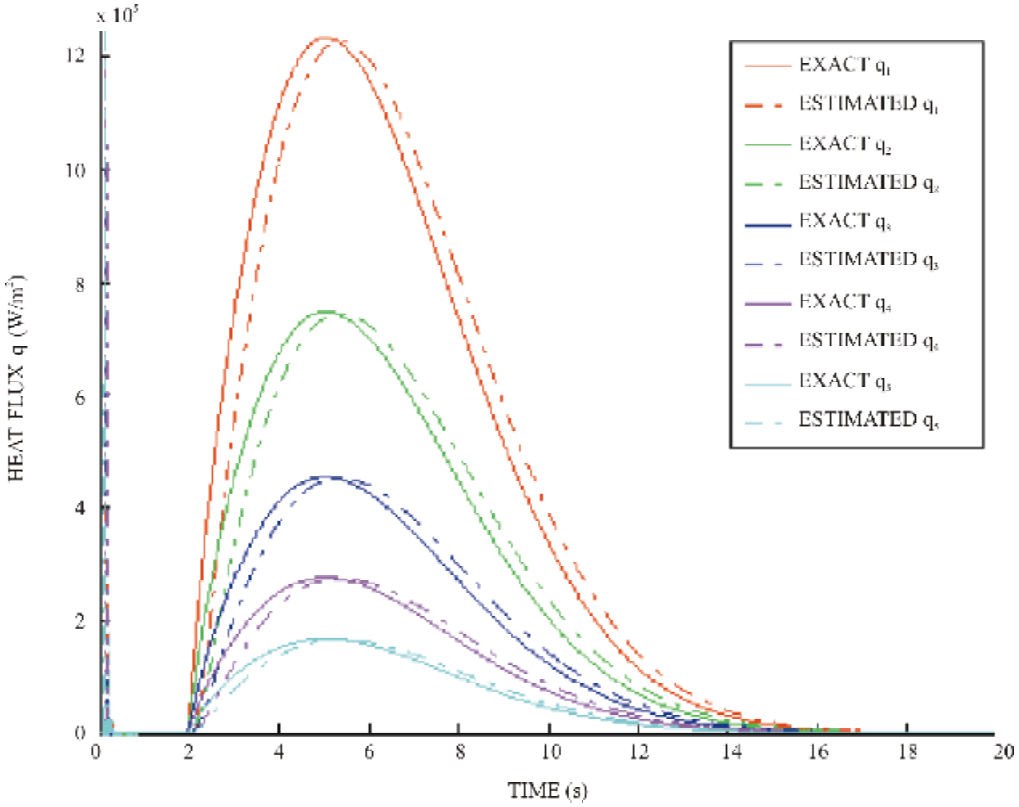


**Figure 8. Inverse estimation for $q(t)$ for example 2 with $\sigma = 0.001$ and $Q = 10$.**

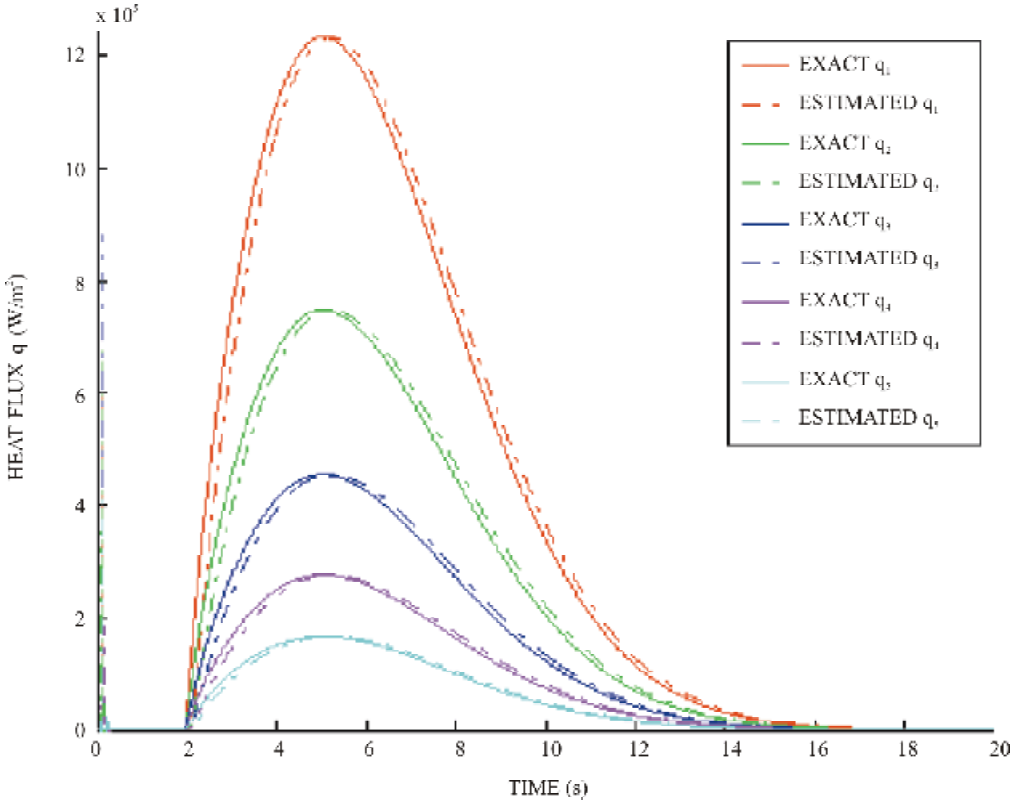


**Figure 9. Inverse estimation for $q(t)$ for example 2 with $\sigma = 0.0001$ and $Q = 1$.**

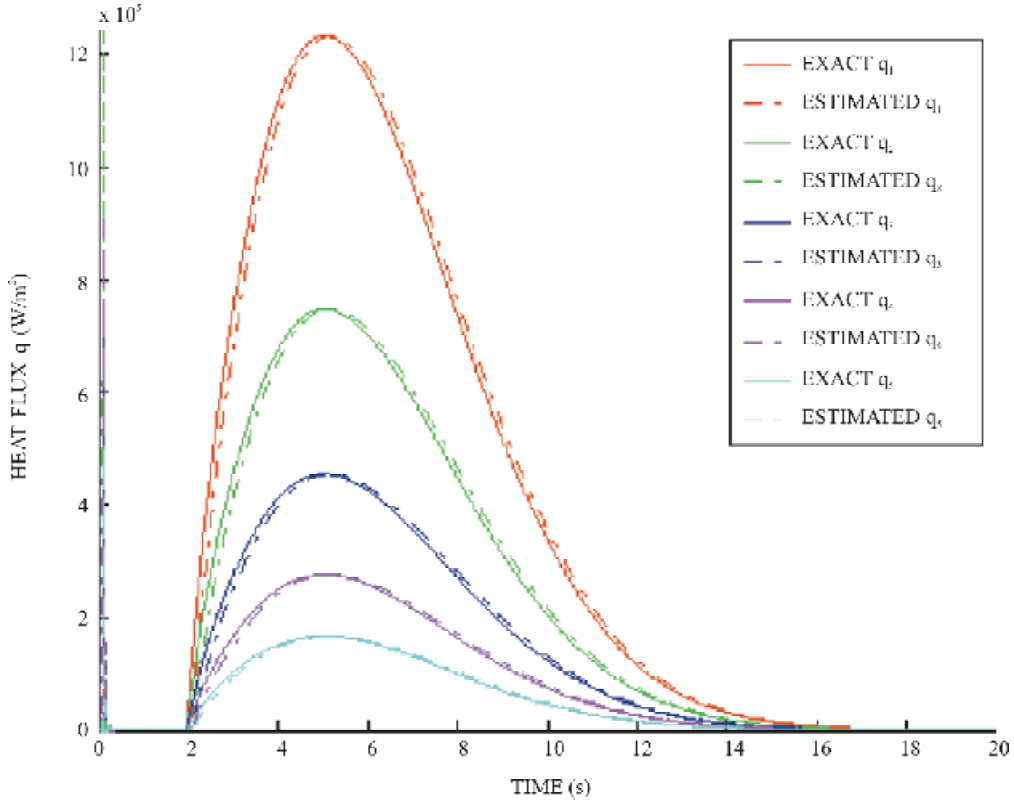


**Figure 10. Inverse estimation for $q(t)$ for example 2 with $\sigma = 0.0001$ and $Q = 10$.**

**Table 1. Relative root mean square error (RRMSE) compare table**

| | | $\Delta t_1$= 0.1s | $\Delta t_1$= 0.01s | $\Delta t_2$= 0.001s |
|---|---|---|---|---|
| | $q_1$ | 0.0117 | 0.0027 | 6.9151e-004 |
| | $q_2$ | 0.0147 | 0.0034 | 8.6868e-004 |
| $\sigma$ =$10^{-2}$, $Q$=1 | $q_3$ | 0.0145 | 0.0035 | 9.0465e-004 |
| | $q_4$ | 0.0134 | 0.0025 | 6.7997e-004 |
| | $q_5$ | 0.0032 | 0.0006 | 5.3625e-005 |
| | $q_1$ | 0.0081 | 0.0011 | 2.9796e-004 |
| | $q_2$ | 0.0096 | 0.0012 | 3.4139e-004 |
| $\sigma$ =$10^{-3}$, $Q$=1 | $q_3$ | 0.0091 | 0.0012 | 3.3514e-004 |
| | $q_4$ | 0.0098 | 0.0011 | 3.0865e-004 |
| | $q_5$ | 0.0012 | 0.0005 | 1.3227e-004 |
| | $q_1$ | 0.0049 | 6.4927e-005 | 6.0416e-006 |
| | $q_2$ | 0.0055 | 6.8465e-005 | 6.8864e-006 |
| $\sigma$ =$10^{-4}$, $Q$=1 | $q_3$ | 0.0052 | 6.3483e-005 | 5.6045e-006 |
| | $q_4$ | 0.0057 | 7.1907e-005 | 7.7857e-006 |
| | $q_5$ | 0.0020 | 5.2549e-005 | 2.9741e-006 |
| | $q_1$ | 0.0110 | 0.0024 | 6.9149e-004 |
| | $q_2$ | 0.0137 | 0.0029 | 8.6869e-004 |
| $\sigma$ =$10^{-2}$, $Q$=10 | $q_3$ | 0.0134 | 0.0030 | 9.0463e-004 |
| | $q_4$ | 0.0129 | 0.0023 | 6.7997e-004 |
| | $q_5$ | 0.0018 | 6.1071e-005 | 5.3606e-005 |
| | $q_1$ | 0.0058 | 2.2952e-004 | 4.7871e-005 |
| | $q_2$ | 0.0065 | 2.3849e-004 | 5.0075e-005 |
| $\sigma$ =$10^{-3}$, $Q$=10 | $q_3$ | 0.0062 | 2.2429e-004 | 4.6245e-005 |
| | $q_4$ | 0.0067 | 2.4219e-004 | 5.1054e-005 |
| | $q_5$ | 0.0023 | 1.9048e-004 | 3.7680e-005 |
| | $q_1$ | 0.0048 | 3.7001e-005 | 8.3940e-007 |
| | $q_2$ | 0.0053 | 3.9820e-005 | 1.5420e-006 |
| $\sigma$ =$10^{-4}$, $Q$=10 | $q_3$ | 0.0050 | 3.6059e-005 | 5.6847e-007 |
| | $q_4$ | 0.0055 | 4.2749e-005 | 2.2980e-006 |
| | $q_5$ | 0.0021 | 2.7469e-005 | 1.4967e-006 |

degradation for the Weibull distribution function heat flux. The estimation results from the proposed method show excellent agreement with the exact value.

*Example 3.* In this example, 15 different levels input-heat flux are modelled by Weibull distribution form; the unknown input-heat flux [$q(z,t)$] is assumed in the following form:

$$q_i(z,t)=\begin{cases}0 & 0\le t<2\\ 2\times10^{8}\times e^{-z_i}\times\dfrac{b}{a}\left(\dfrac{t-2}{a}\right)^{b-1}\times e^{-\left(\frac{t-2}{a}\right)^{b}} & 2\le t<t_f\\ a=4.8, b=1.8 & i=1,2,3,.....14,15\\ z_i=1+0.2\times(i-1) & i=1,2,3,.....14,15\end{cases} \tag{42}$$

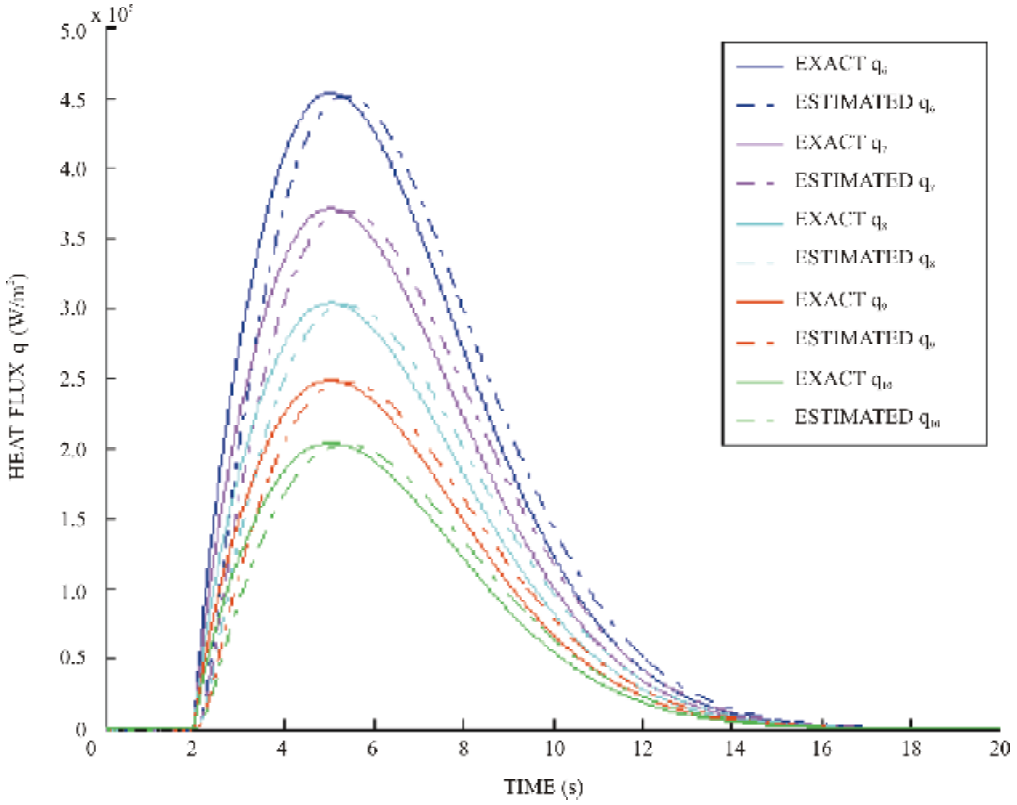


**Figure 11. Inverse estimation for $q_{6\text{-}10}(t)$ for example 3 with σ = 0.001 and $Q$ = 10.**

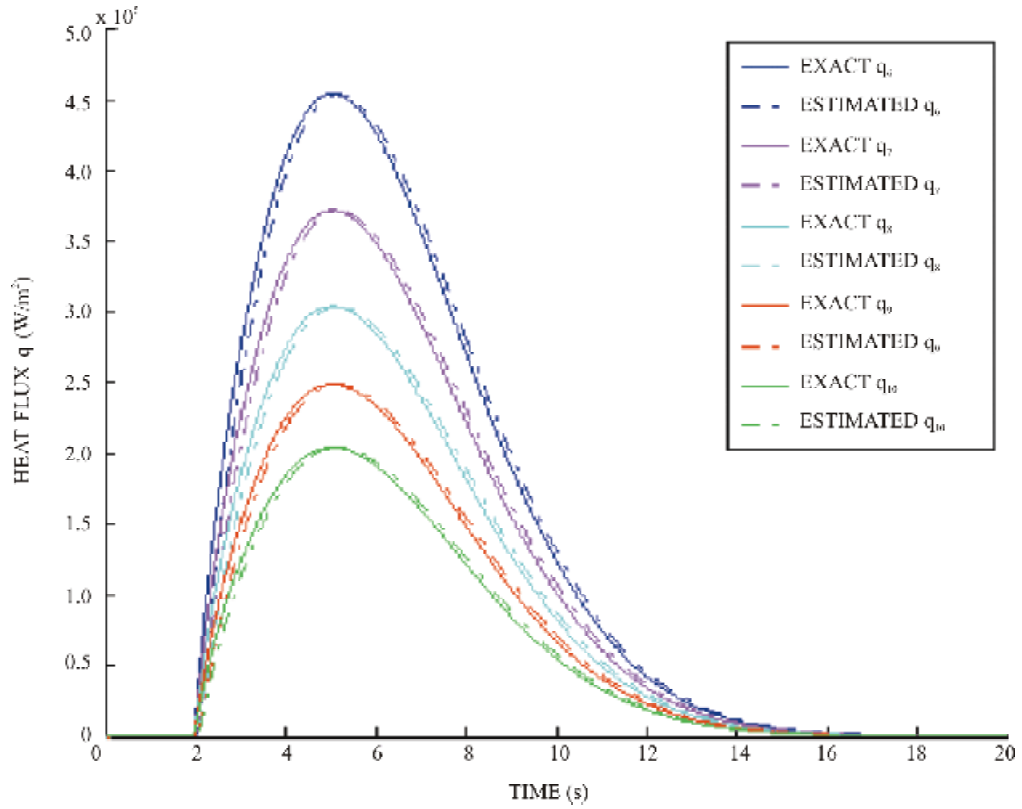


**Figure 12. Inverse estimation for $q_{11\text{-}15}(t)$ for example 3 with σ = 0.0001 and $Q$ = 10.**

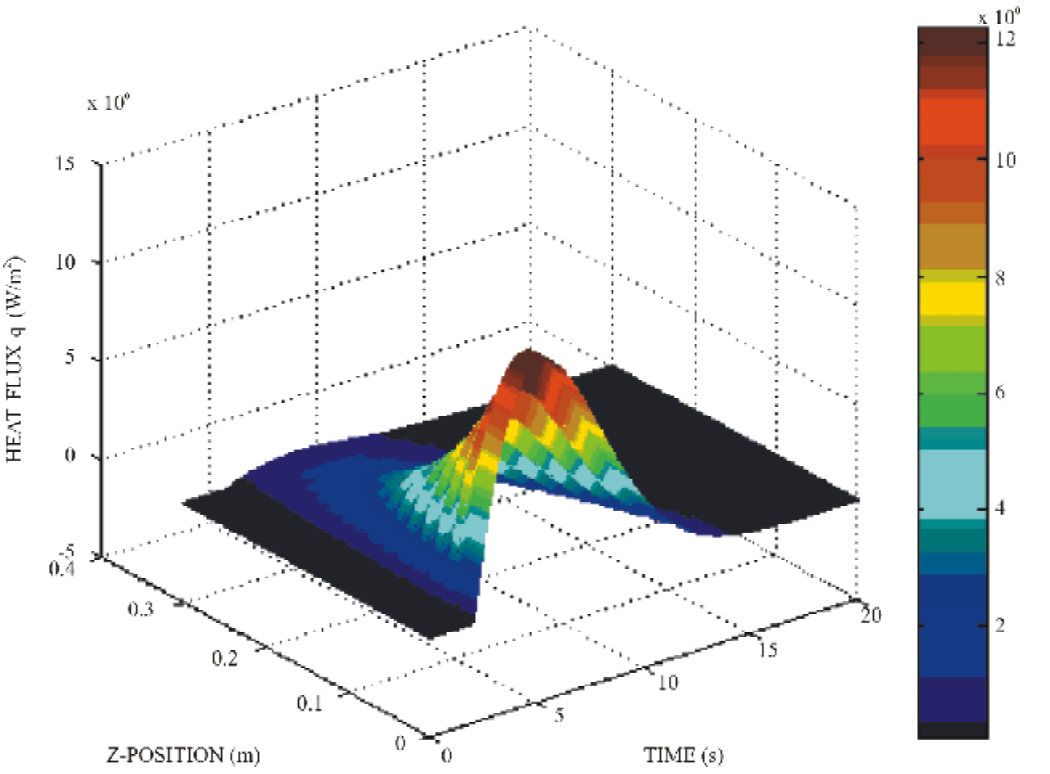


**Figure 13. 3-D heat flux (*z*, *t*, *q*) for example 3.**

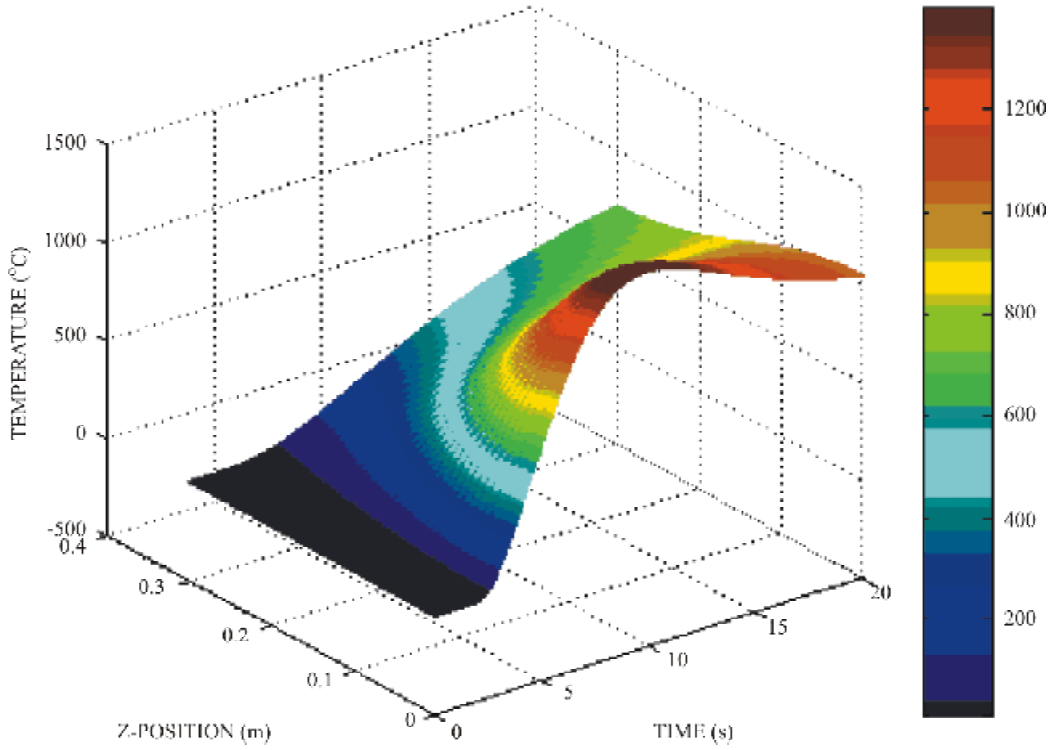


**Figure 14. 3-D temperature (*z*, *t*, *T*) for example 3 in the inner wall.**

In this example, 15 different level input heat flux decreases with exponent form in different positions, and enlarge 10 times of heat flux compared to *example 2*. The sensors location are at $r = R_0$, node 12,24,36,...156,168,180. One chooses the measurement error, $\sigma$ = 0.001 and $\sigma$ = 0.0001, process noise variance $Q$=10 and the sampling time interval $\Delta t$ = 0.01s. In this case, one plots the $\hat{q}_{6-10}(t)$. The estimated $\hat{q}_{6-10}(t)$ is shown in Figs 11-12, 3-D heat flux ($z$,$t$,$q$), and inner wall temperature ($z$,$t$,$T$) in Figs 13-14. In this example, one can find the heat flux magnified 1 order and the result is also excellent.

The above simulation results demonstrate that the proposed method has good performance in tracking unknown heat flux cases that vary with the time and the $z$-axial location, and the algorithm is capable of dealing with online 2-D gun barrel hollow cylinder IHCP.

## 5. CONCLUSIONS

An online methodology, based on the input estimation method including the finite element scheme, has been developed to estimate the unknown input heat flux that varies with the time and the $z$-axial location on 2-D gun barrel. The results of the simulation show that this method using the measured temperature on 2-D gun barrel outer surface can precisely estimate the unknown time-varying heat flux, and the temperature field distribution on the chamber in real-time. The proposed method is effective for IHCP, it can be useful in making quick and efficient identification of unknown heat flux on the inner surface. In the future, it can be further applied to other gun life prediction and relative nondestruction tests.

## REFERENCES

1. Ward, J.R.; Brosseau, T. L. & Grollman, B.B. Heat transfer in guns-determination of friction factor from heat input measurements. US Army Armament Research and Development Command, US Army Ballistic Research Laboratory, Aberdeen Proving Ground, MD, 1981. Report No AD–A105430.

2. Fisher, R.M; Szirmae, A. & Kamdar, M.H. Metallographic studies of erosion and thermo-chemical cracking of cannon tubes. US Army Armament Research & Development Command, Benet Weapons Laboratory, DRDAR-LCB-TL Watervliet, NY, 1983. Report No.AD–A135816.

3. Blecker, J.M. Small arms gun barrel thermal experimental correlation studies. Research Directorate, SARRI-LR GEN Thomas J. Rodman Laboratory Rock Island Arsenal, Rock Island, IL, 1974. Report No.AD–786509.

4. Caveny, L.H. Steel erosion produced by double base, triple base, and RDX composite propellants of various flame temperature. US Army Armament Research and Development Command, Large Caliber Weapon Systems Laboratory, Dover, New Jersey, 1980. Report No.AD–A092344 .

5. Conroy, P.J. Gun tube heating. US Army Ballistic Research Laboratory, Aberdeen Proving Ground, MD, 1991. Report No. BRL-TR-3300; Report No.AD–A243265.

6. Gerber, N. & Bundy, M. Heating of a tank gun barrel: Numerical study. US Army Ballistic Research Laboratory, Aberdeen Proving Ground, MD, 1991. Report No. BRL-TR-3932; Report No. AD– A241136.

7. Gerber, N. & Bundy, M. Effect of variable thermal properties on gun tube heating. US Army Ballistic Research Laboratory, Aberdeen Proving Ground, MD, 1992. Report No. BRL-TR-3984, Report No.AD–A253066,.

8. Gerber, N. & Bundy, M. Cross-barrel temperature difference due to wall thickness variation. US Army Ballistic Research Laboratory, Aberdeen Proving Ground, MD, 1993. Report No. ARL-TR-100, Report No.AD–A262509.

9. Gerber, N. & Bundy, M. Gun barrel heating with heat input during projectile passage. *Journal of Ballistics*, 1995, **12**, (4), 267-81.

10. Tian, Q; Wu, J; Fan, X; & Zhang, Y; Finite difference technique for heat conduction in multilayer gun barrels. *Acta Armament AR*II, 2000, **21**(4).

11. Long-miao, Chen & Lin-fang, Qian. Study on erosion and service life of composite material Barrel. *Acta Armament AR*II, 2005, **26**(6).

12. Bass, B.R. & Ott, L.J. A finite element formulation of the two-dimensional inverse heat conduction problem. *Adv. Comp. Technol*., 1980, **2**, 238-48.

13. Yoshimura, T. & Ituka, K. Inverse heat conduction problem by finite element formulation. *Int. J. Syst. Sci*., 1985, **16**, 1365-376.

14. Ling, X.; Keanini, R.G. & Cherukuri, H.P. A non-iterative finite element method for inverse heat conduction problems. *Int. J. Numer. Meth. Engg.*, 2003, **56**(9), 1315-334.

15. Tuan, P.C.; Ji, C.C.; Fong, L.W. & Huang, W.T. An input estimation approach to online two-dimensional inverse heat conduction problems. *Numer. Heat Transfer, Part B*, 1996, **29**, 345-63.

16. Reddy, J.N. Applied functional analysis and variational in engineering. Malabar, Florida, 1991.

17. Larry, J.S., Applied finite element analysis. East Lansing, Michigan, 1976.

18. Jazwinski, A.H. Stochastic processes and filtering theory. Academic Press, New York, 1970.

19. Wu, B. & Xia, W. Analysis of heat transfer in actively cooled compound gun barrel. *J. China Ord. Soc*., 2005, **1**(1), 29-36.

20. Chan, Y.T.; Hu, A.G. & Plant, J.B. A Kalman filter-based tracking scheme with input estimation. *IEEE Trans. Aero. Elec. Syst.*, 1979, **AES-15**, 237-44.

21. Chen, T.C. & Tuan, P.C. Input estimation method including finite element scheme for solving inverse heat conduction problems. *Numer. Heat Transfer, Part B*, 2005, **47**, 1-14.

22. Kuo, C.M.; Du, R.H.; Lin, C.Y. & Yu, P.S. The comparison of potential evapotranspiration estimation using remote sensing data from AVHRR and MODIS images. *J. Taiwan Water Conservancy*, 2005, **53**(4).

**Contributors**

**Dr Tsung-Chien Chen** obtained his MS and PhD both from the Chung Cheng Institute of Technology, Taiwan, in 1994 and 2005. He had served in the Department of Systems Engineering at the Chung Cheng Institute of Technology, Taiwan, from 1991-2006. Presently, he is Associate Professor in the Department of Power Vehicle and Systems Engineering of Chung Cheng Institute of Technology. His research areas include: Estimation theory, inverse problems, control theory, tracking system, optimal control of heat-dissipating, etc.

**Mr Chiun-Chien Liu** obtained his MS (System Engineering) from the Chung Cheng Institute of Technology, Taiwan, in 2001. His major research interests include: Estimation theory, control theory application, tracking system, etc.